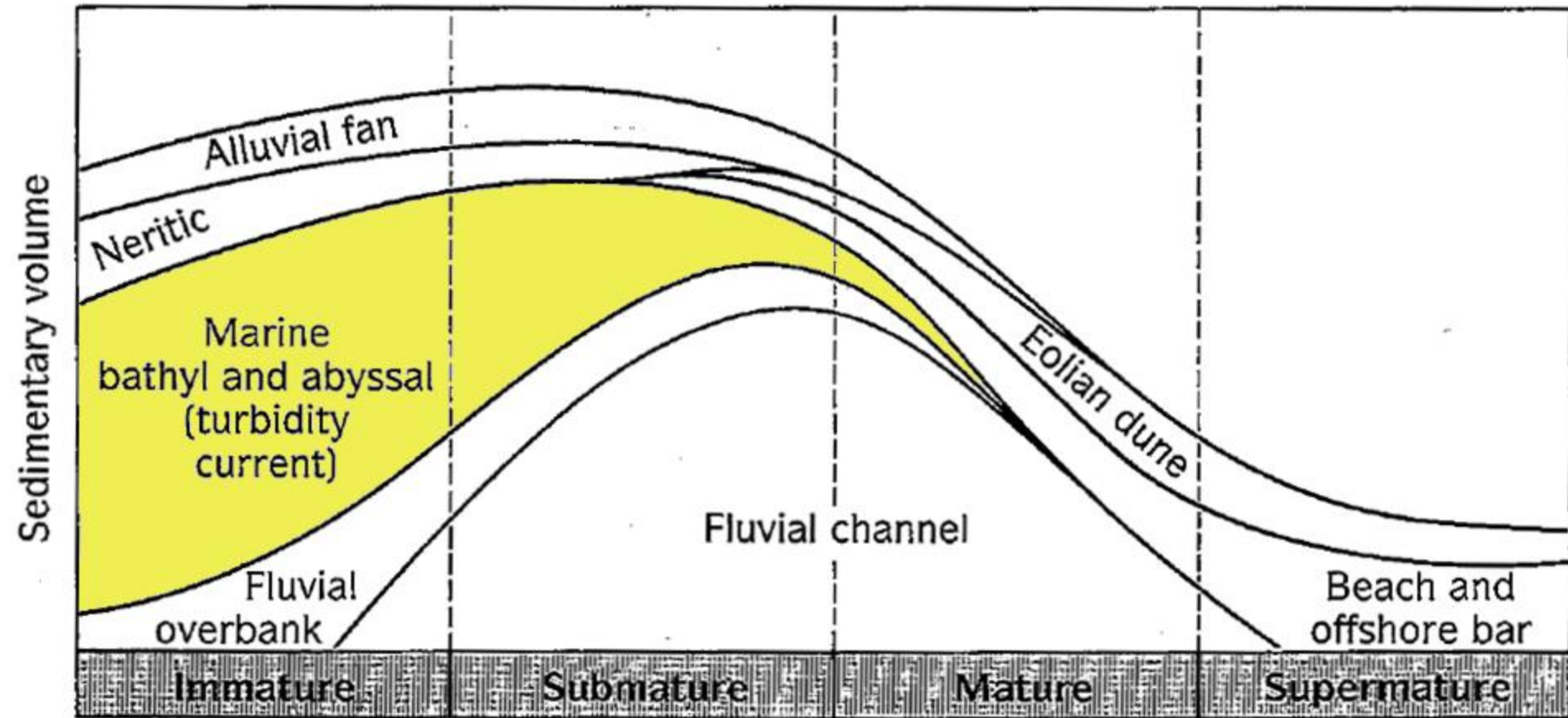




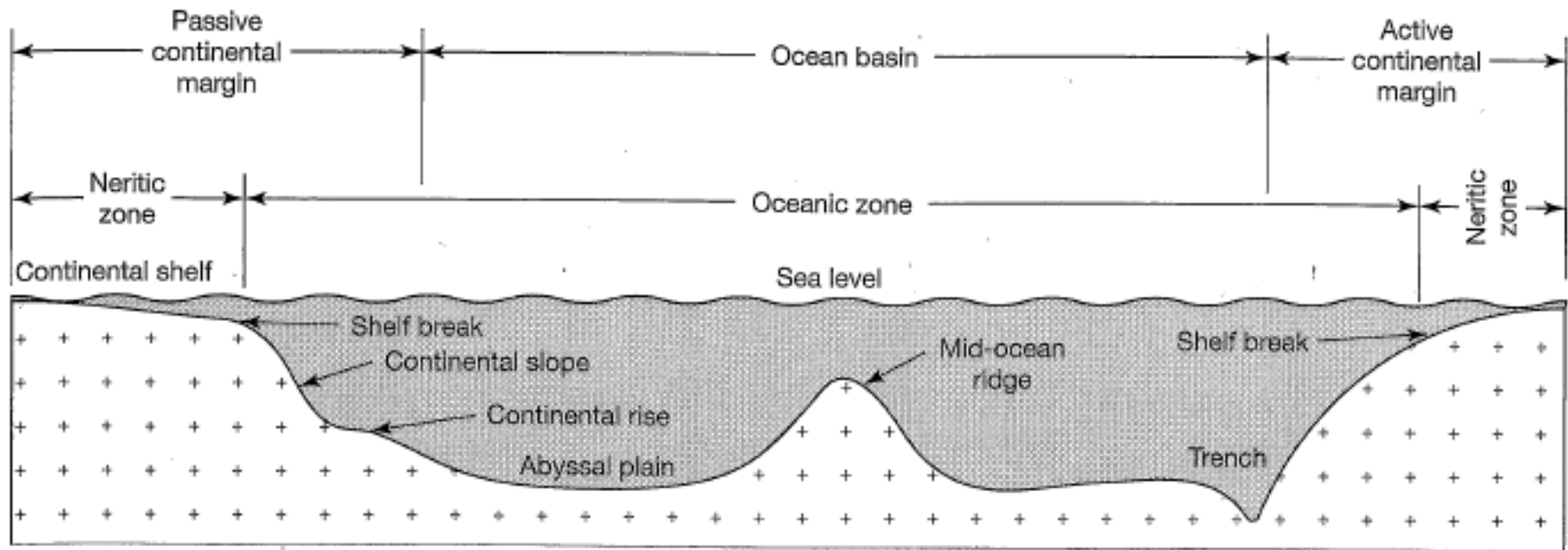
**GEOL-201**  
**Marginal to Deep Marine**  
**Depositional Environments**

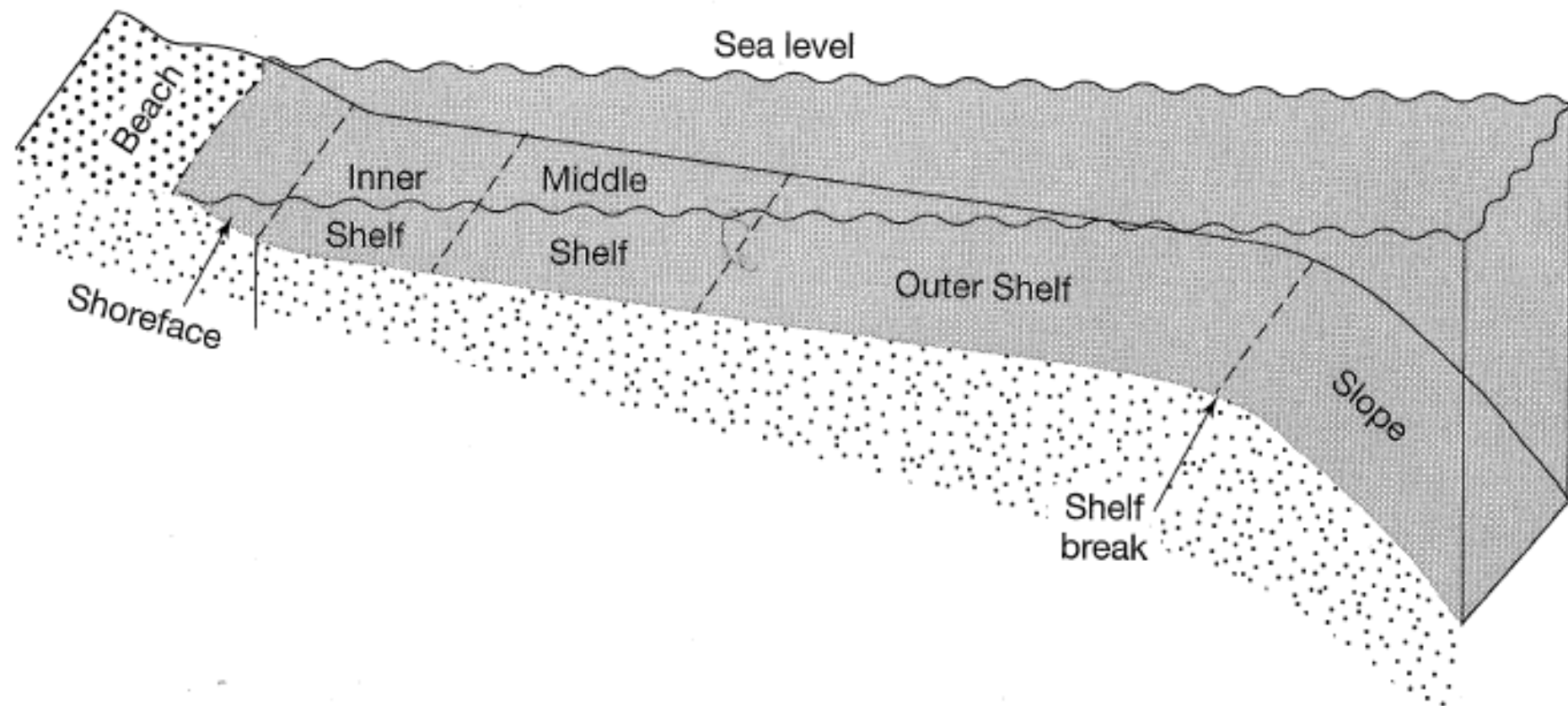


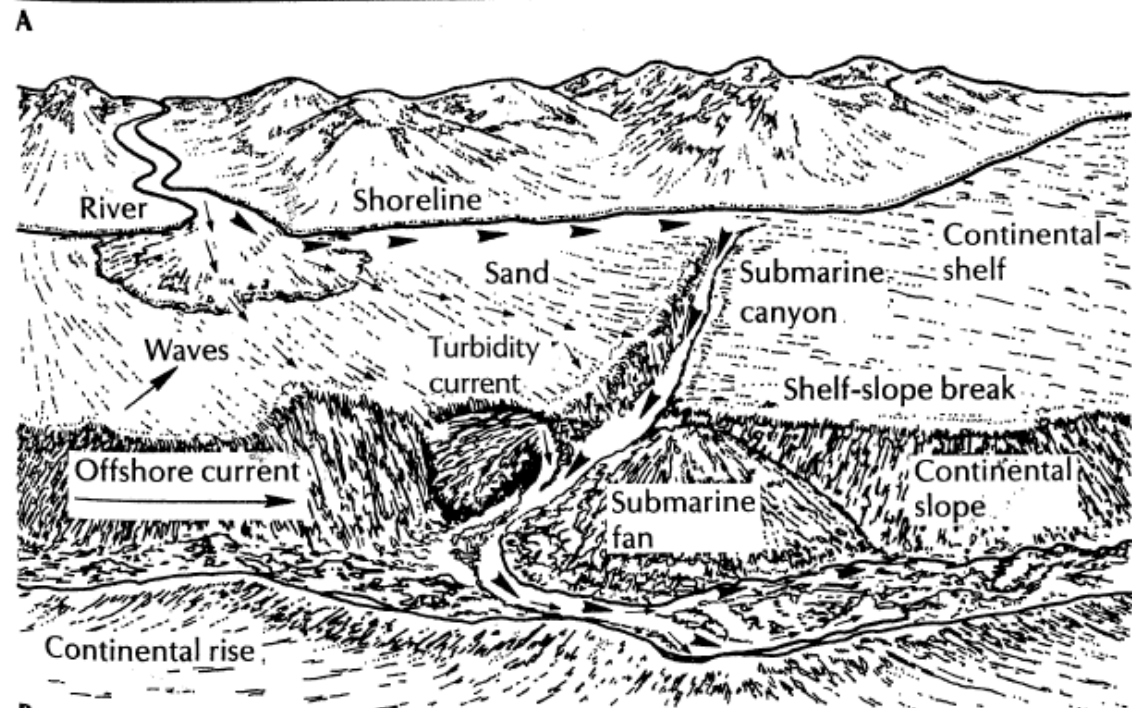
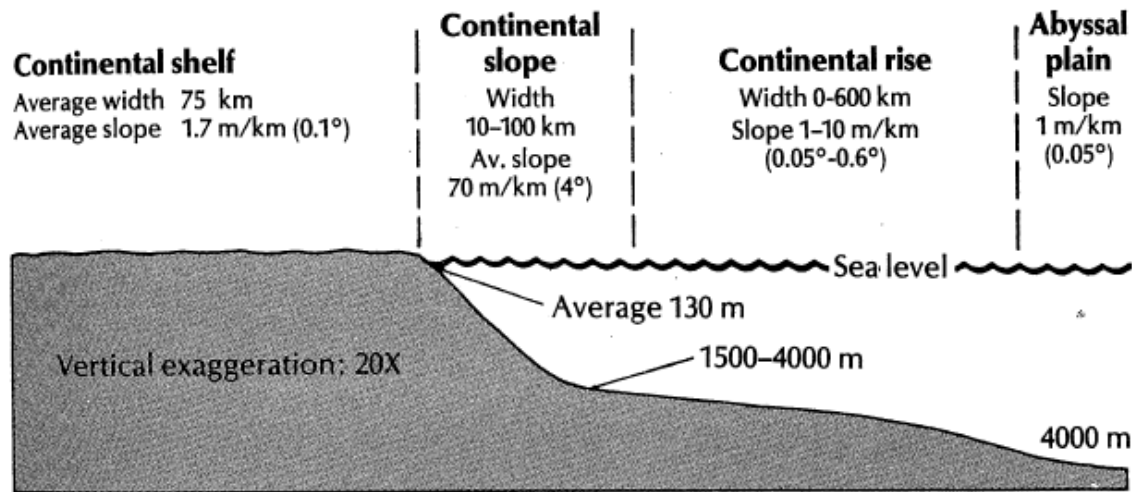
# Sandstones



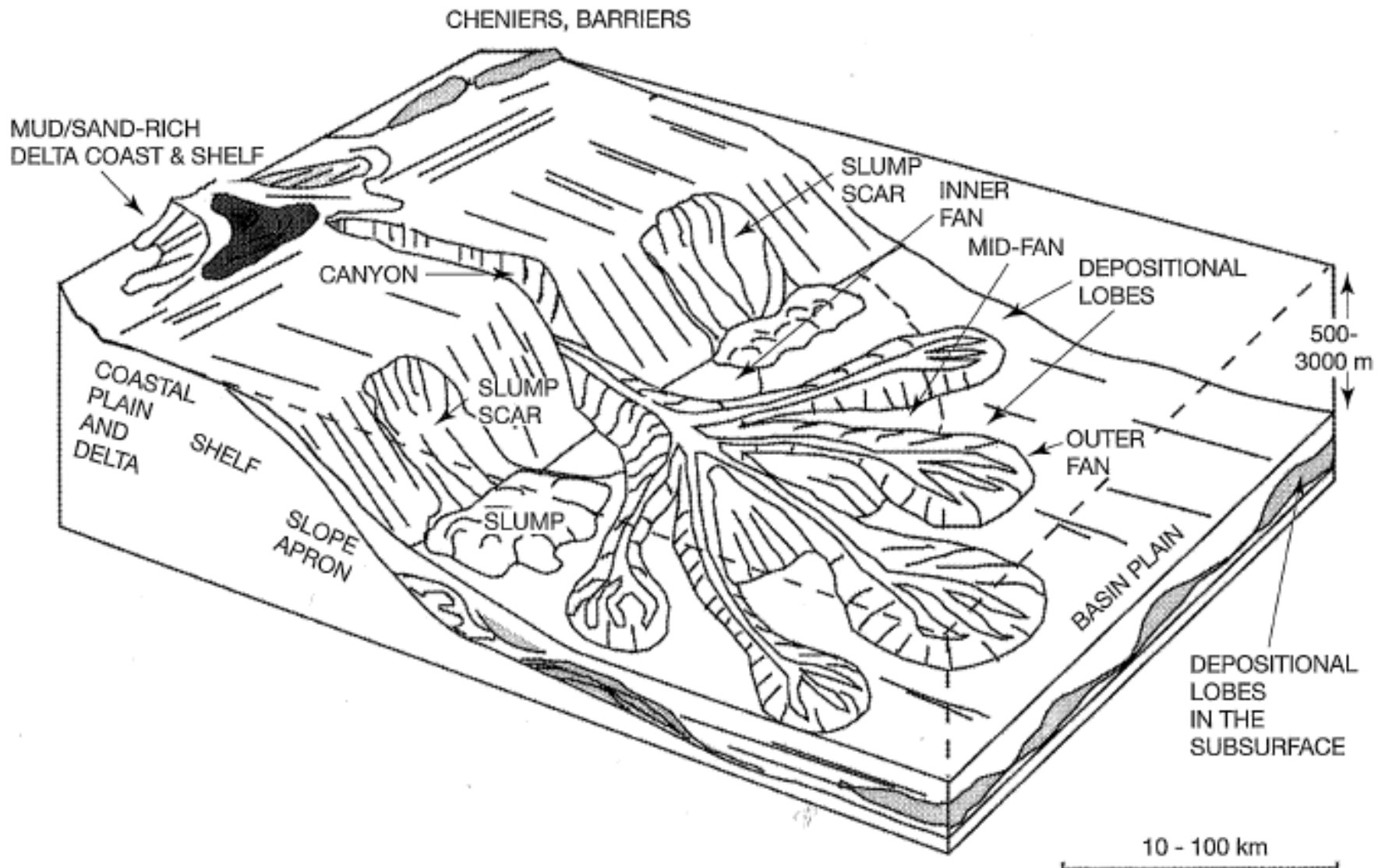
# Ocean bathymetry



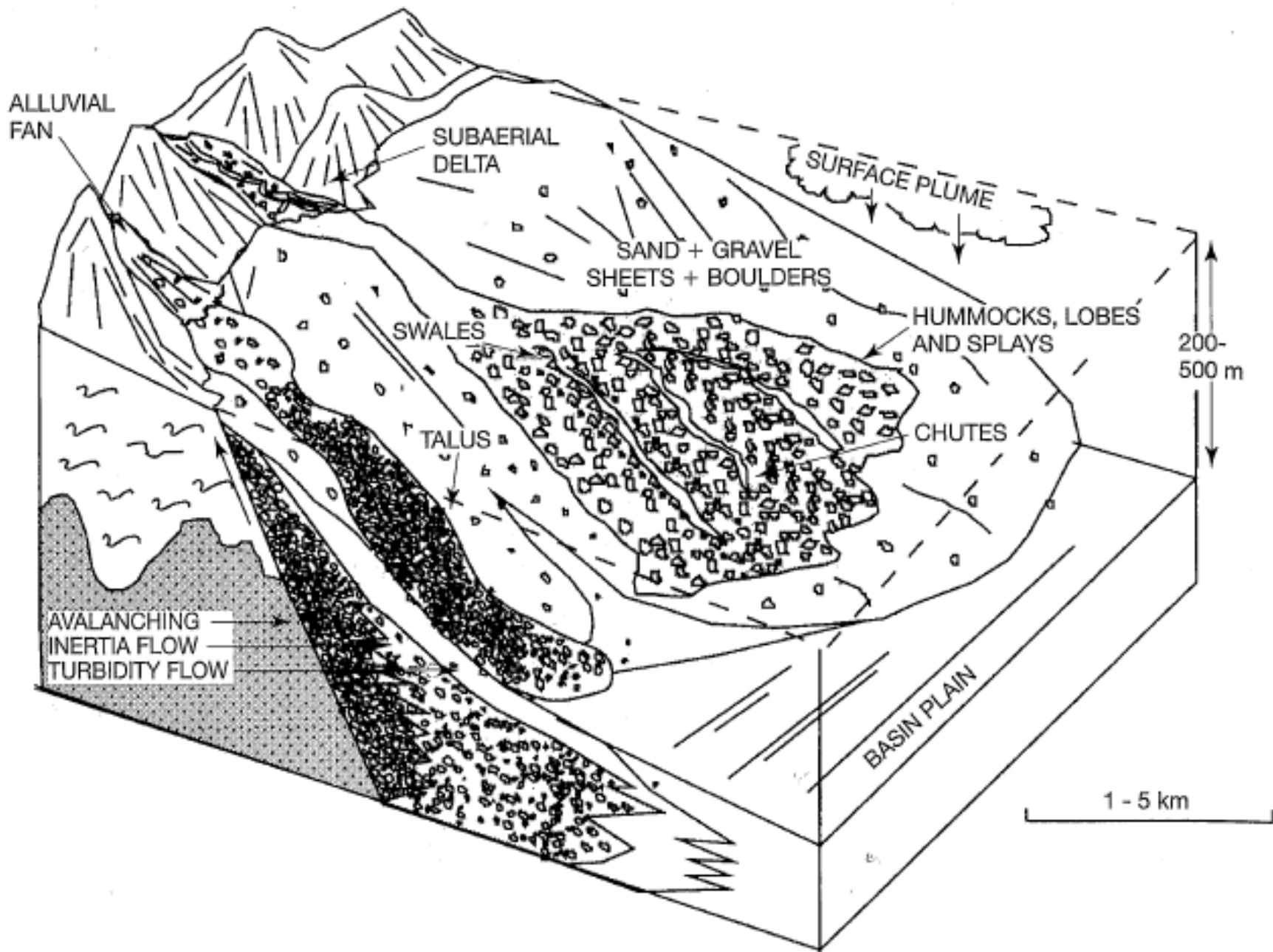




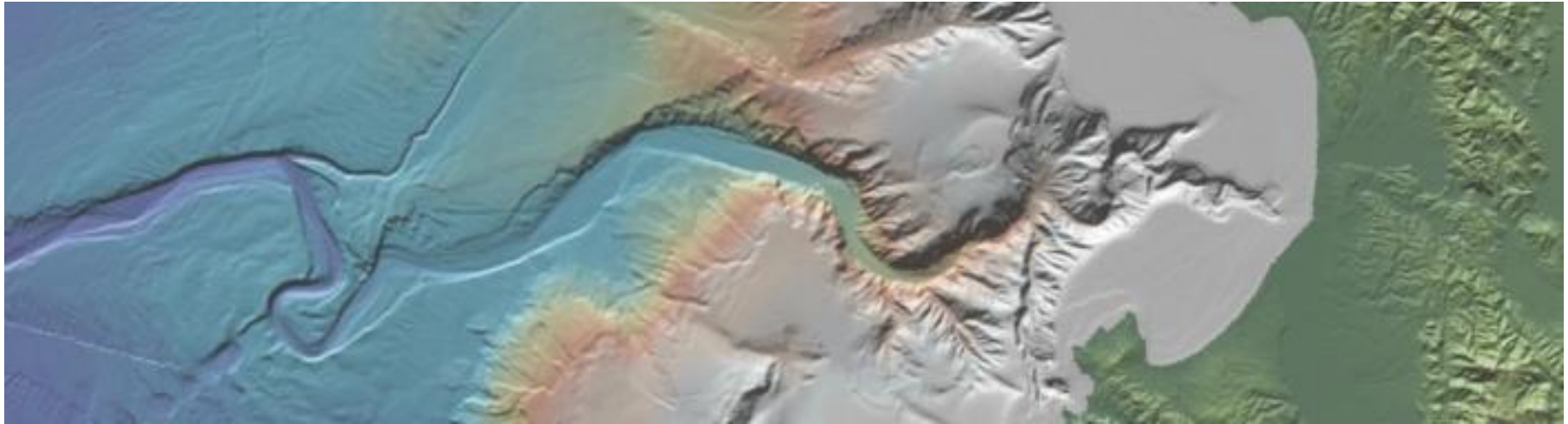
# Sand-rich sub-marine fan



# Gravel-rich sub-marine fan



# Modern Submarine Fans

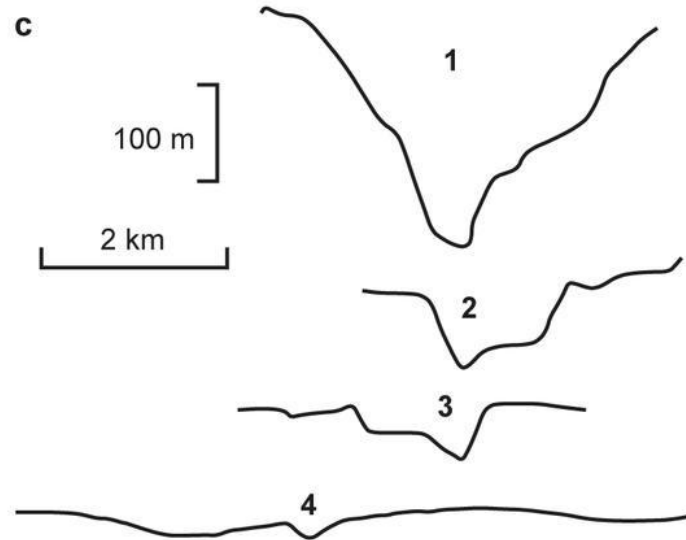
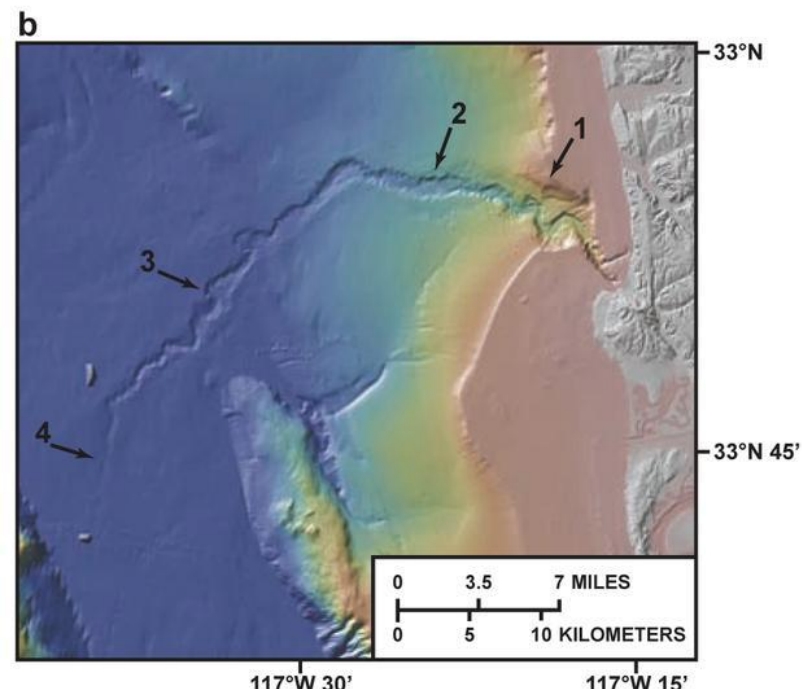
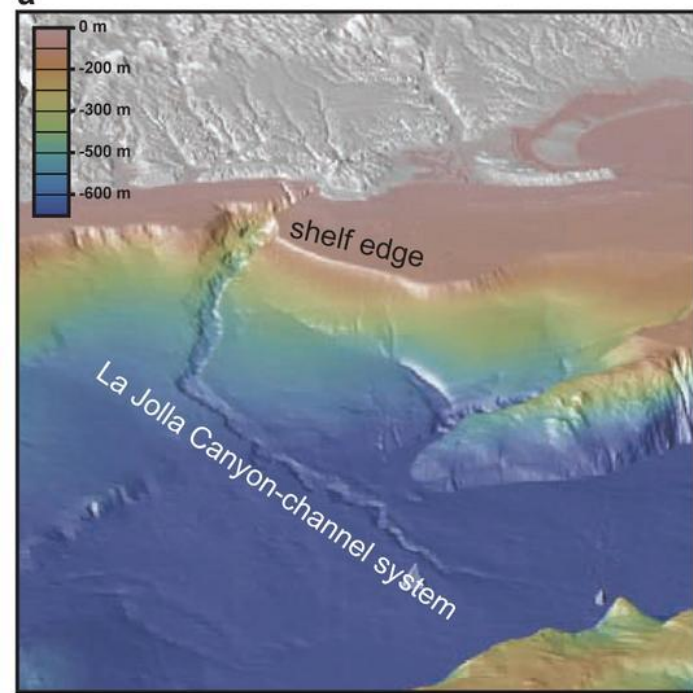


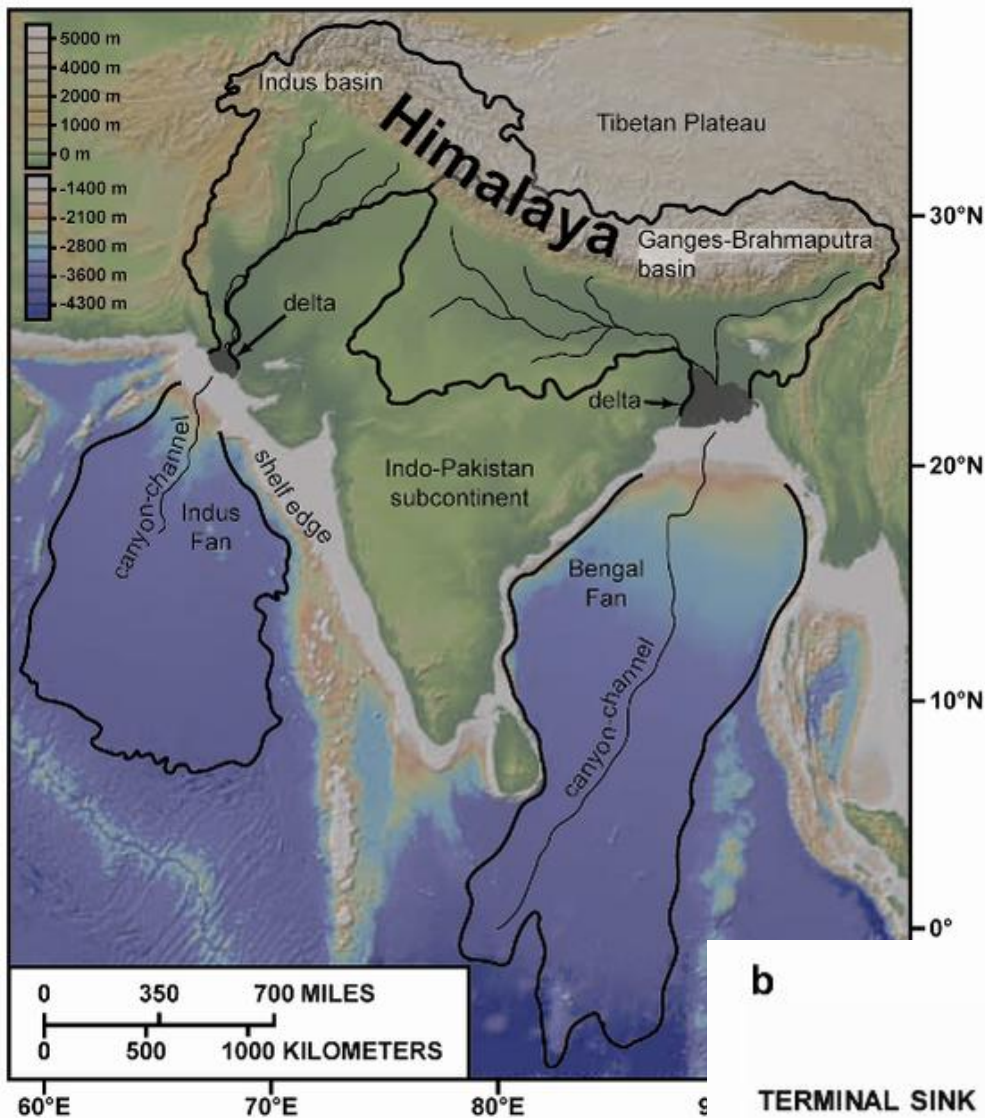
Covault, J. A. (2011) Submarine Fans and Canyon-Channel Systems: A Review of Processes, Products, and Models. *Nature Education Knowledge* 2(12):4

<http://www.nature.com/scitable/knowledge/library/submarine-fans-and-canyon-channel-systems-a-24178428>

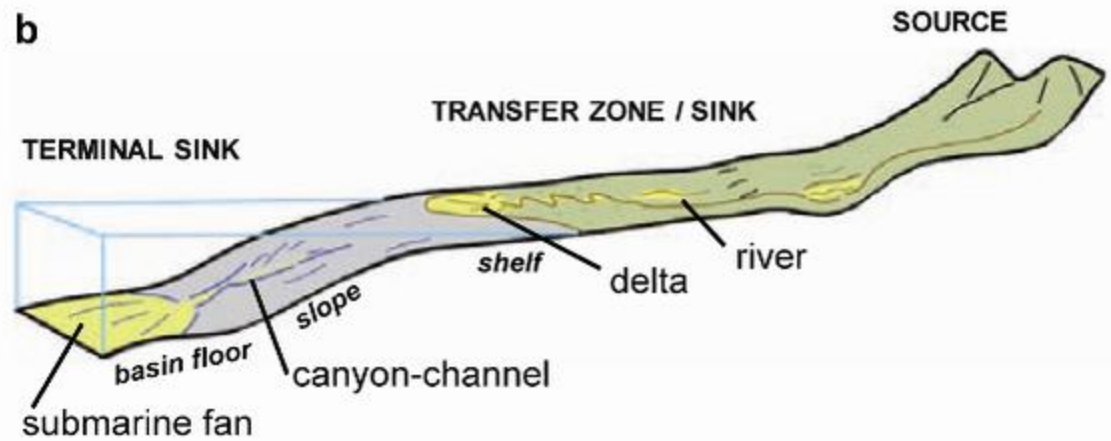


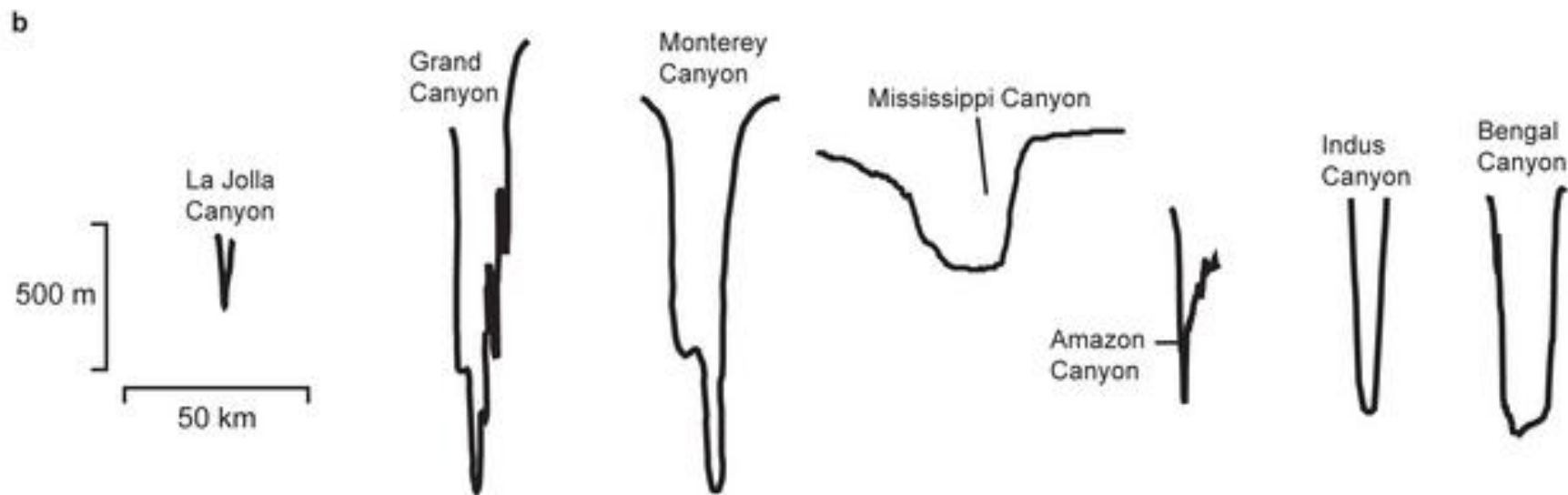
# La Jolla Canyon (southern California)



**a**

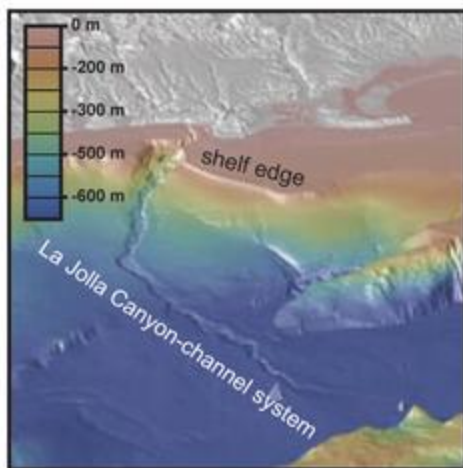
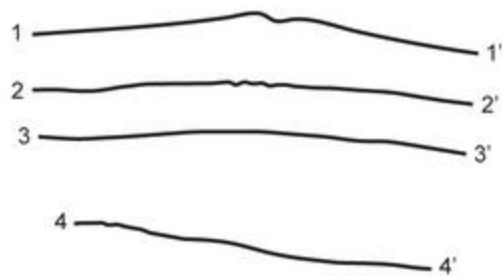
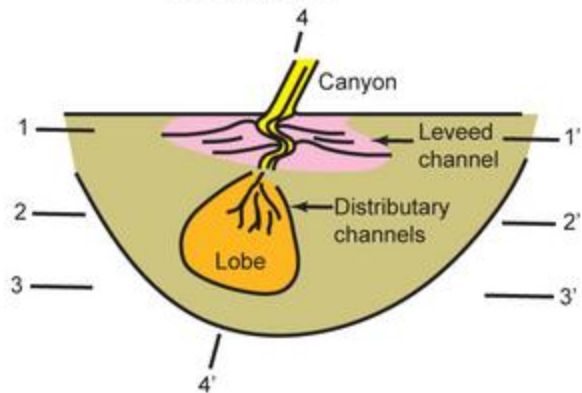
# Himalayas - Indus and Bengal Fans

**b**



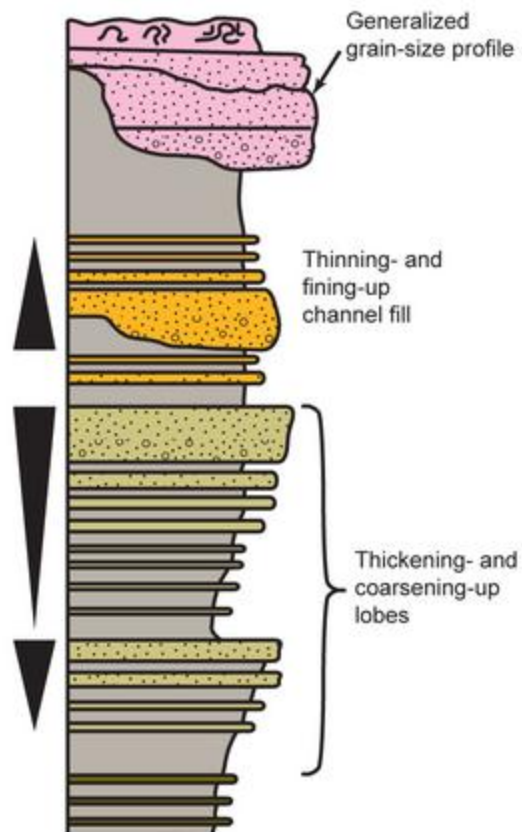
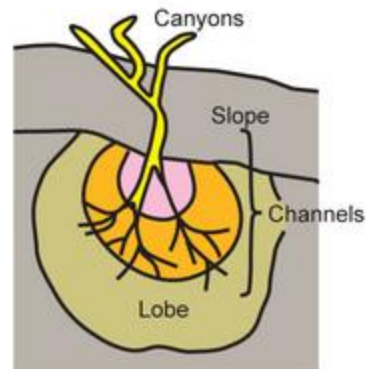
## a Modern fan model

Normark (1970)



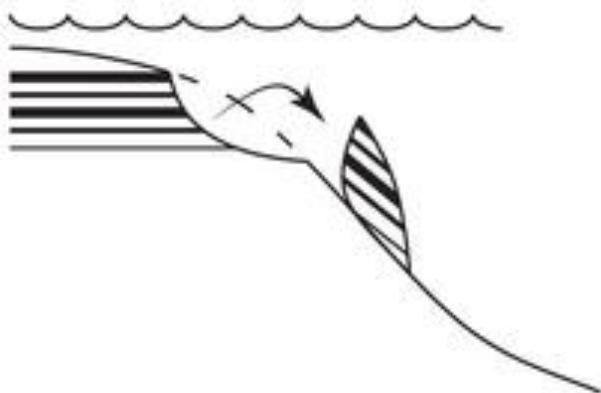
## b Ancient fan model

Mutti and Ricci Lucchi (1972)

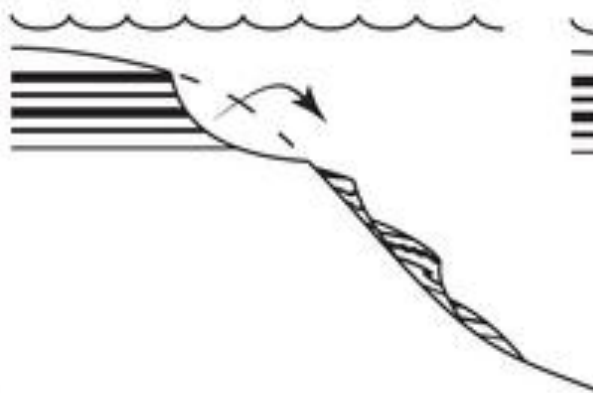




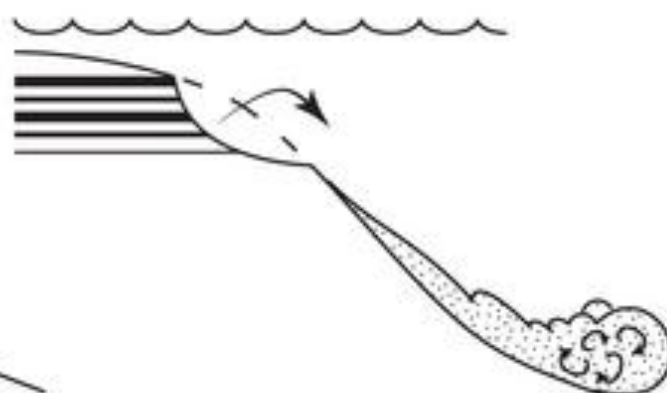
**a** Slide



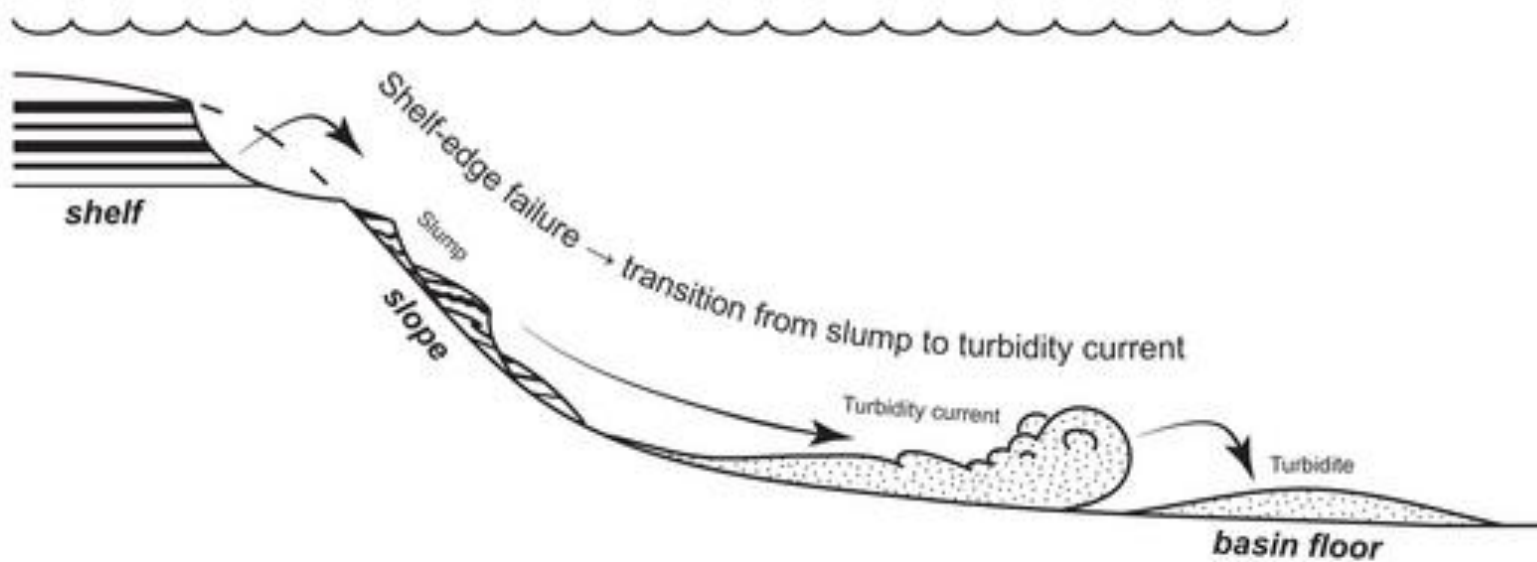
**b** Slump

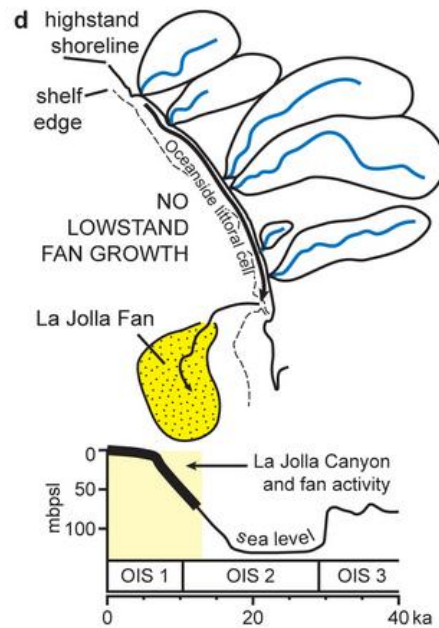
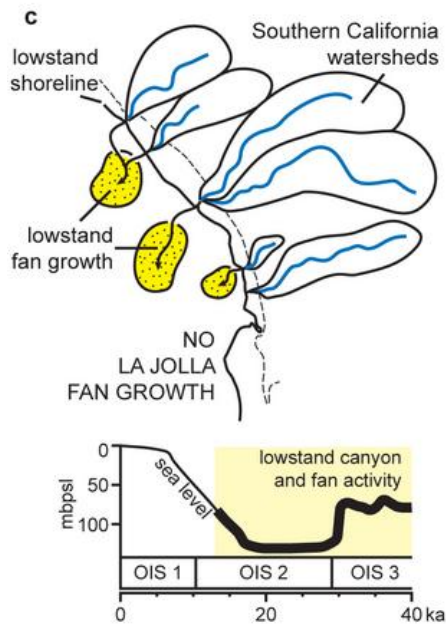
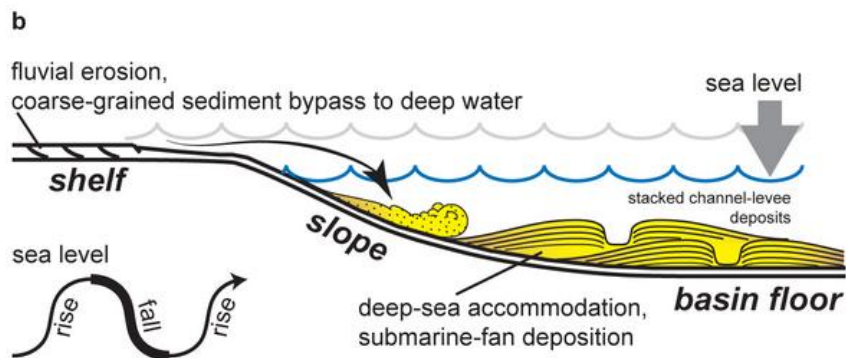
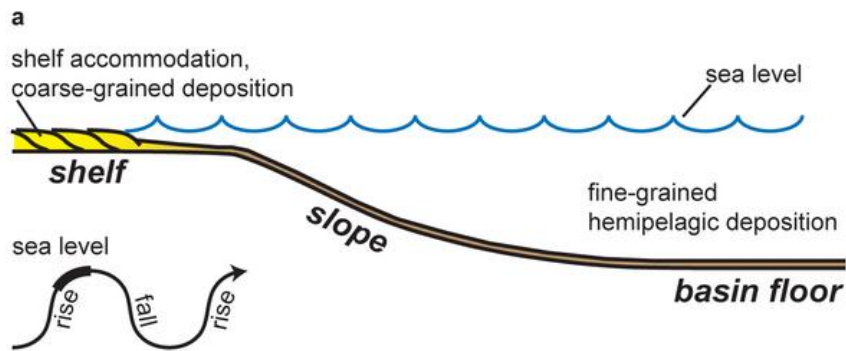


**c** Flow



**d**





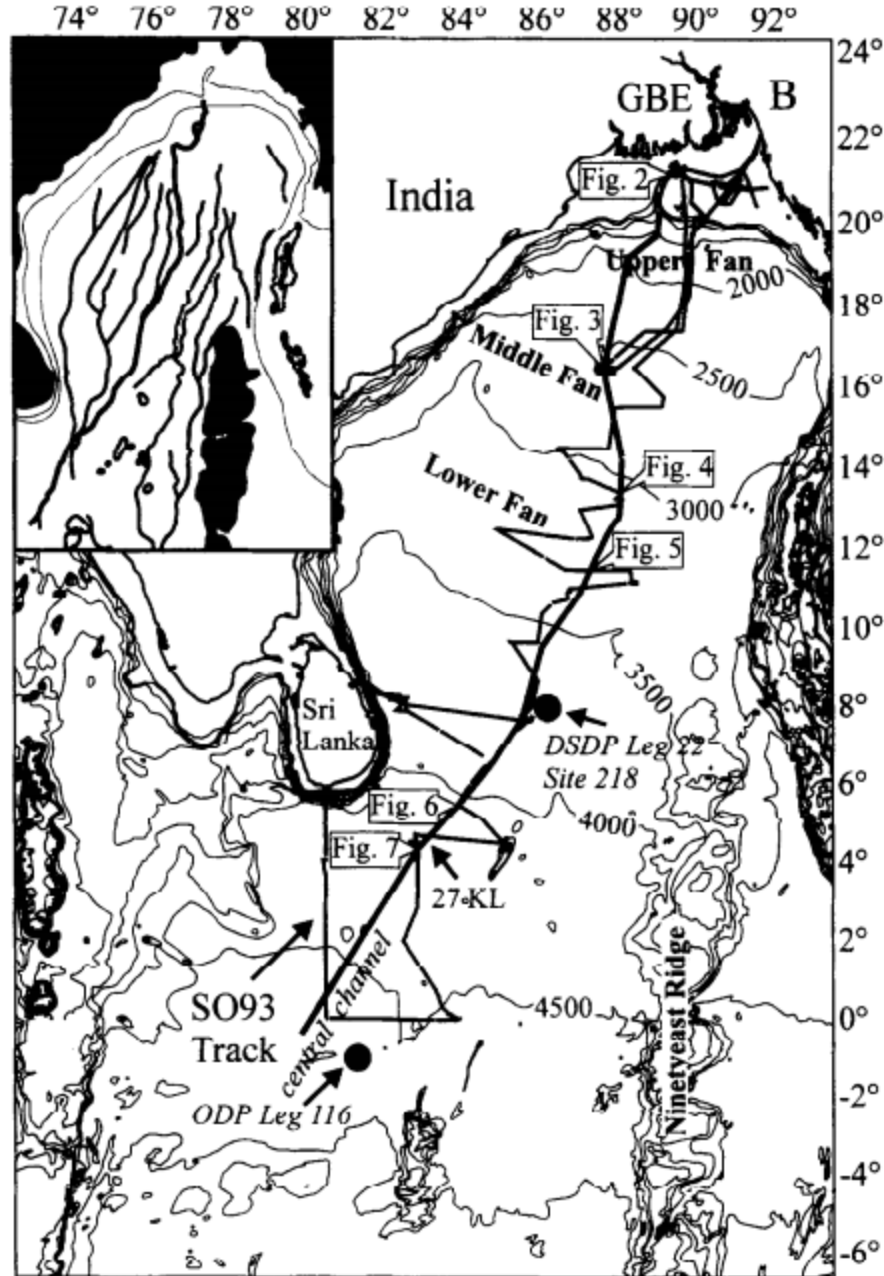
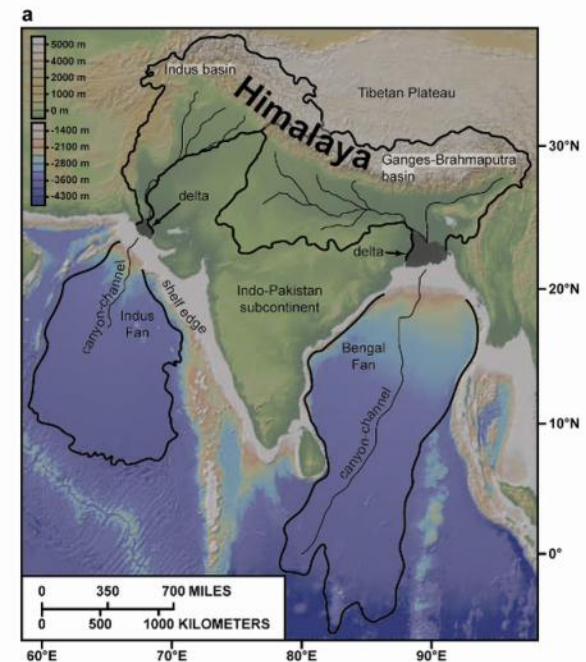


Fig. 1. Map of the Bengal Fan with SO 93 cruise track. PARASOUND data have been obtained along the entire cruise track. The inset map shows correlated channels (redrawn from Emmel and Curray, 1985). The active channel is marked by the thicker black line. B = Bangladesh, GBE = Ganges-Brahmaputra Estuary.

Christian Hiibschner , Volkhard Spiel, Monika Breitzke , Michael E. Weber

The youngest channel-levee system of the Bengal Fan: results from digital sediment echosounder data

Marine Geology 141 (1997) 125-145



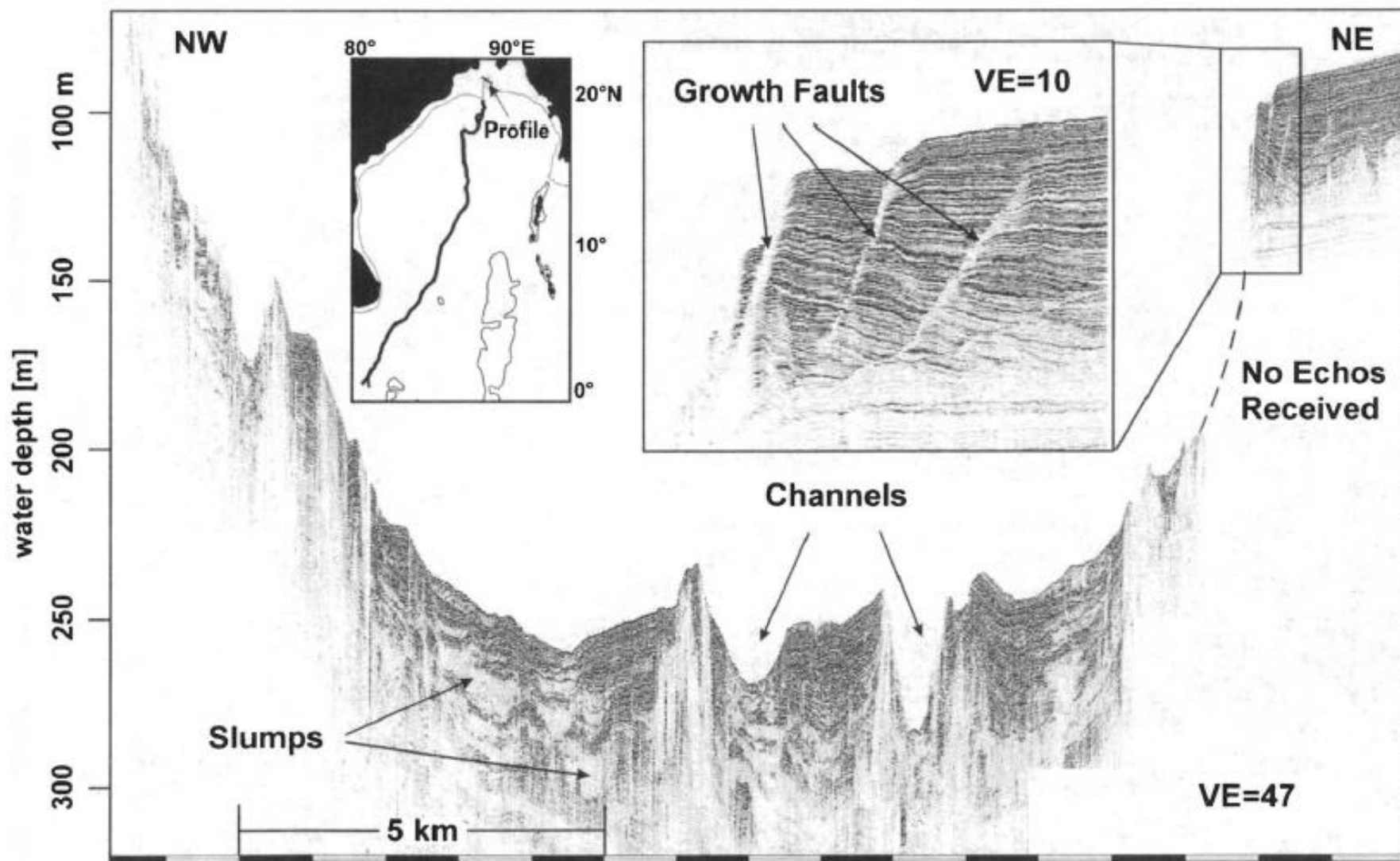


Fig. 2. PARASOUND section of the Swath of No Ground. For location, refer to Fig. 1. The data gap at the eastern flank of the canyon is caused by the steep slope angle. Channels are incised into the bottom of the canyon. *VE* = vertical exaggeration.



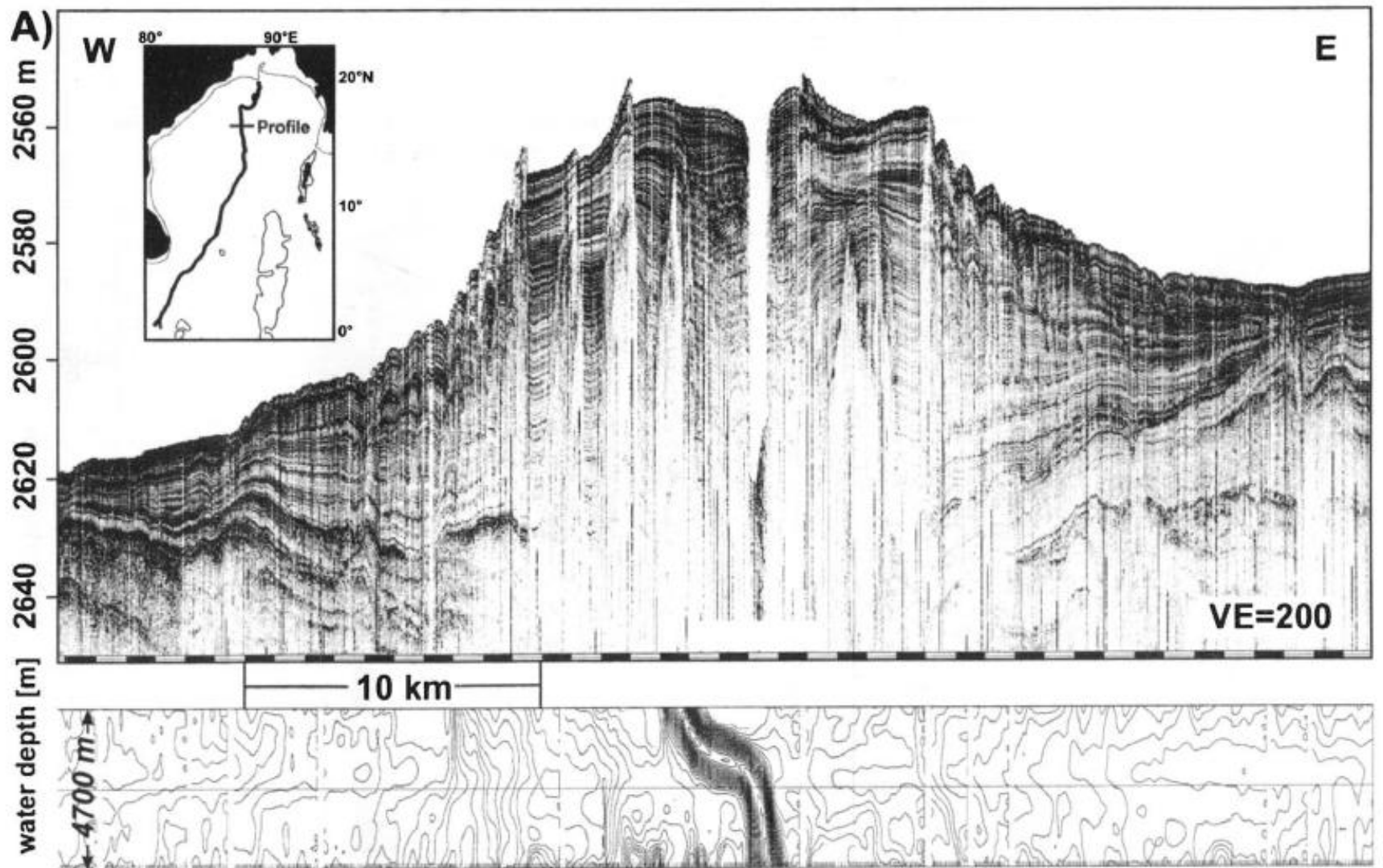


Fig. 3. (A) PARASOUND section of the youngest channel-levee system in the middle fan at 16°30'N with HYDROSWEEP data. (B) Interpreted section. For location, refer to Fig. 1. Italic number refers to swath width. Piston cores 117–120 KL are marked with arrows. The locations of 119–120 KL are projected onto the levees, which have been collected outside the profile. See text for discussion. *aCLS*=abandoned channel-levee system, *dl*=distal layer, *ich*=intra-channel highs, *VE*=vertical exaggeration.

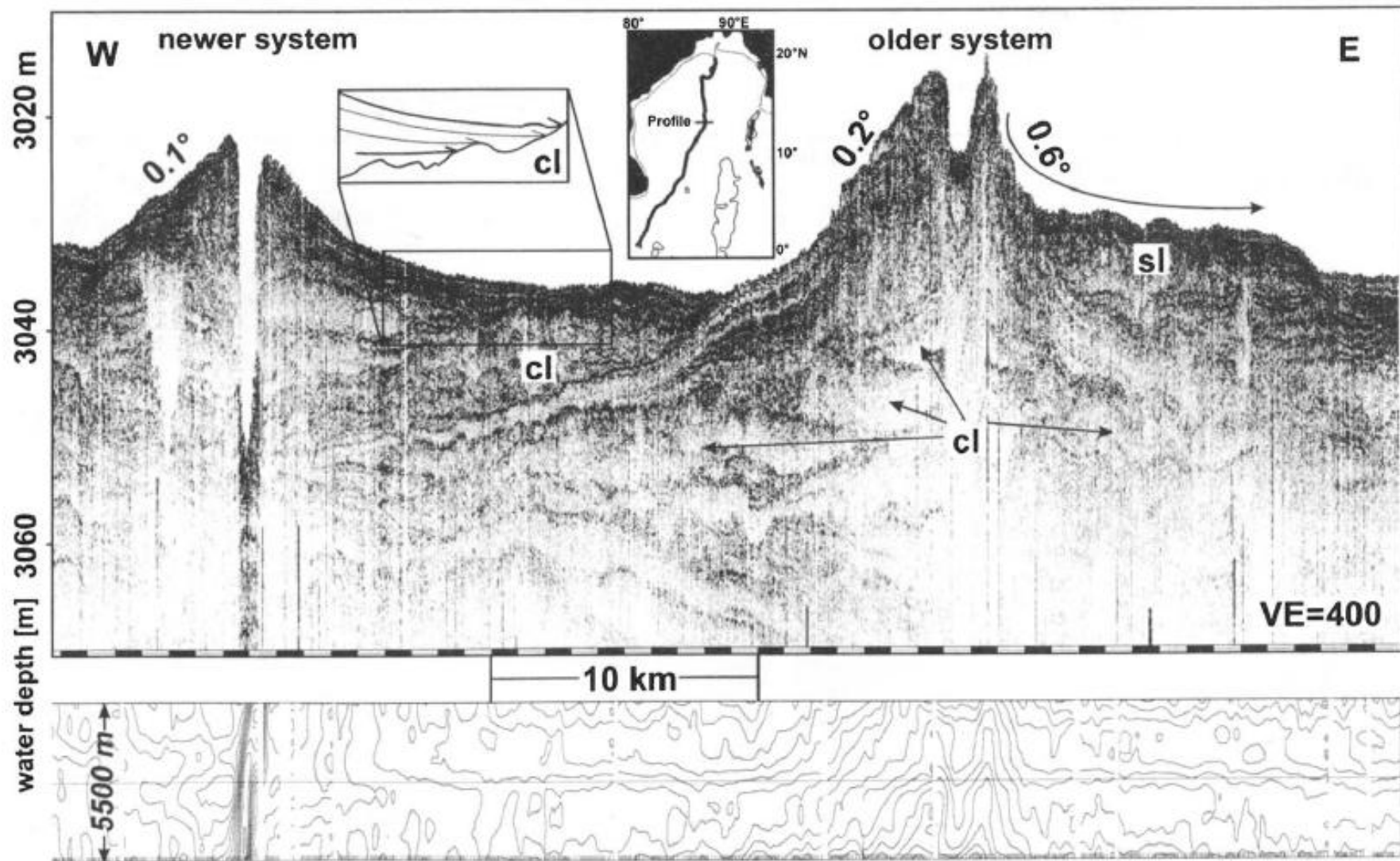


Fig. 4. PARASOUND section and HYDROSWEEP data of the youngest channel-levee system in the lower fan at 13°30'N. For location, refer to Fig. 1. Italic number refers to swath width. The westernmost of the two observed channels represents the recent channel; *cl*=chaotic layer, *sl*=slump, *VE*=vertical exaggeration.

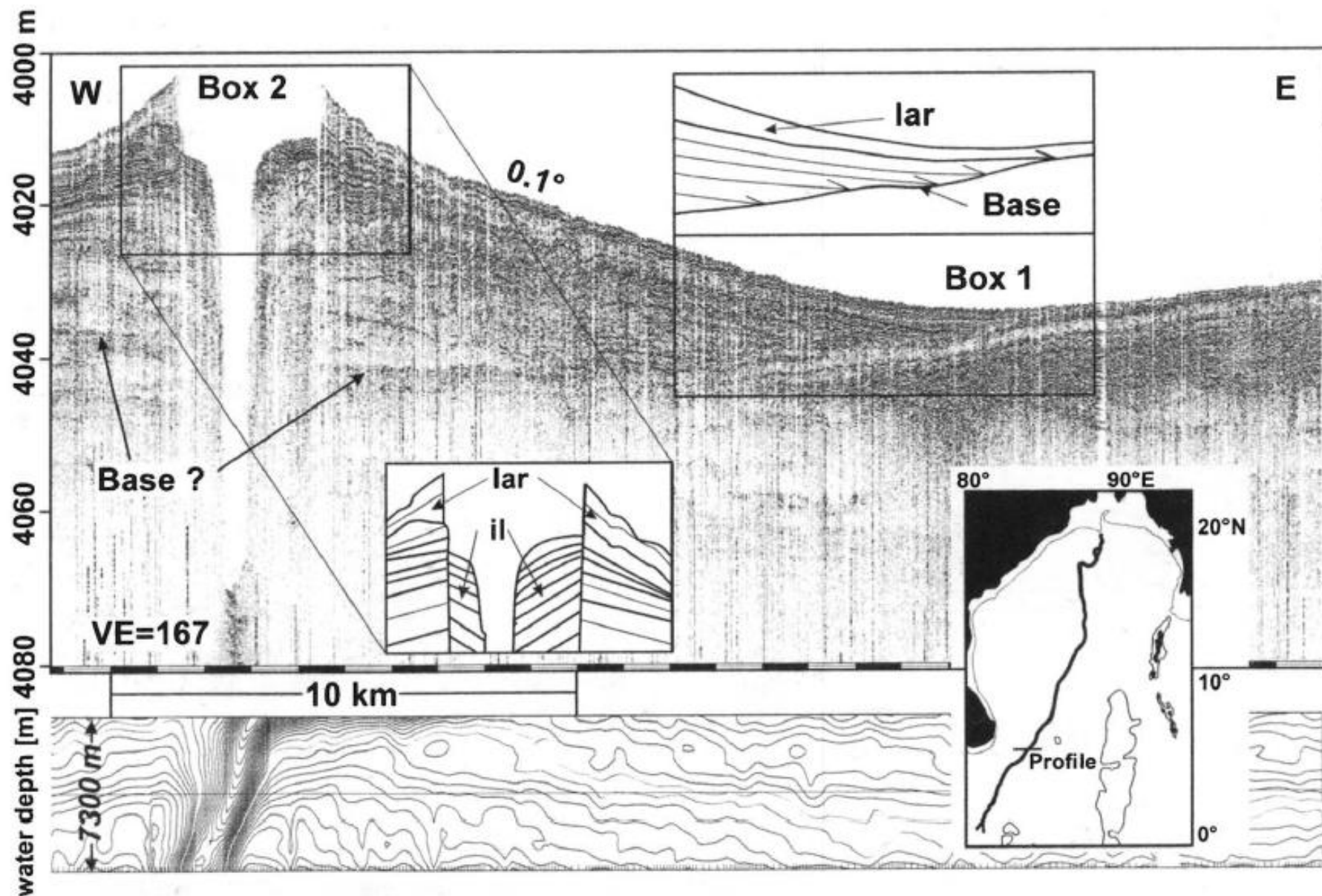


Fig. 6. PARASOUND section with HYDROSWEEP data of the youngest channel-levee system in the lower fan at 5°30'N. For location, refer to Fig. 1. Italic number refers to swath width. The interpreted base of the levees is marked by arrows. The channel has been constricted by the deposition of sediment at the inner levee flank; *lar* = low amplitude reflections, *il* = inner levees, *VE* = vertical exaggeration.

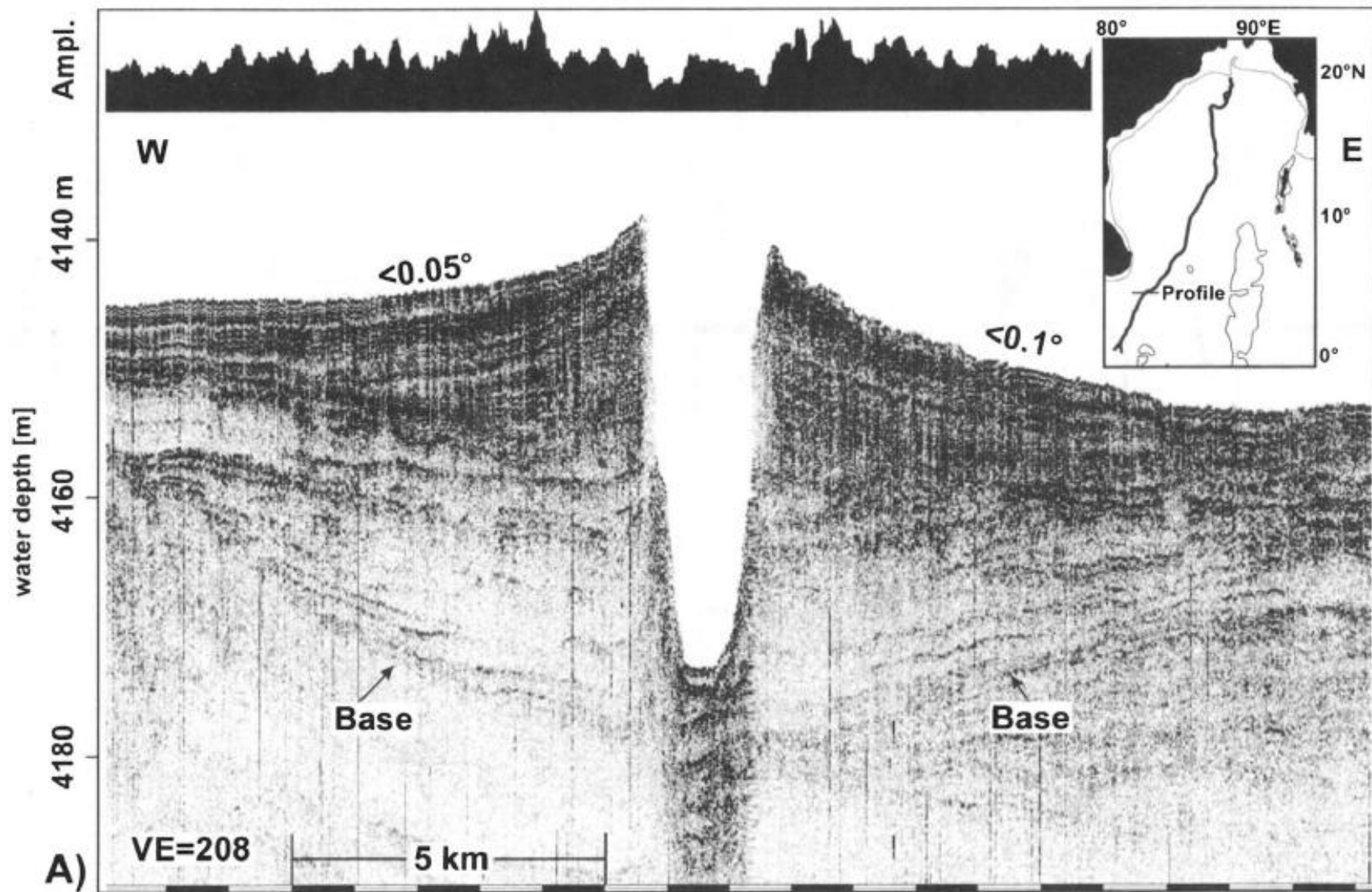


Fig. 7. (A) PARASOUND section of the youngest channel-levee system in the lower fan at  $4^{\circ}30'N$ , (B) line drawing. For location, refer to Fig. 1. The entire system is separated into two vertical units. The lower unit generally exhibits a diffuse reflection pattern with some divergent reflections onlapping at the convex shaped base. Distinct dipping reflections of the outer side of the upper unit terminate as a downlap on to the surface which separates the two units. The maximum reflection amplitudes are plotted at the top:  $VE$ =vertical exaggeration.



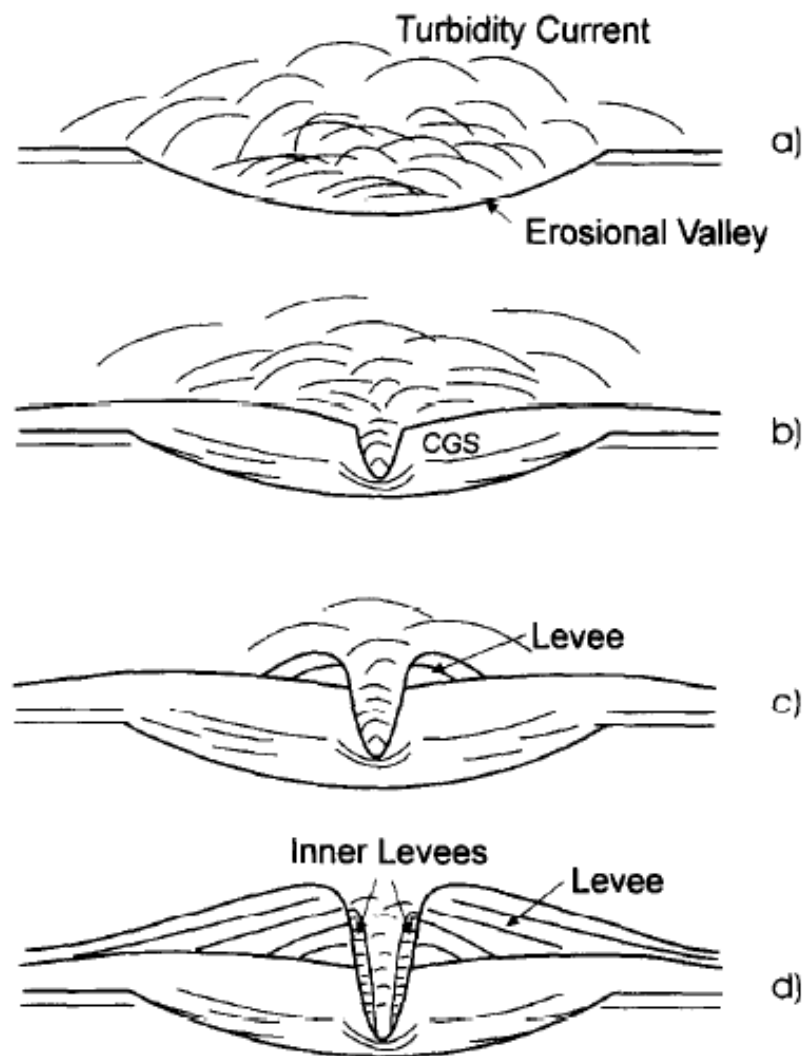
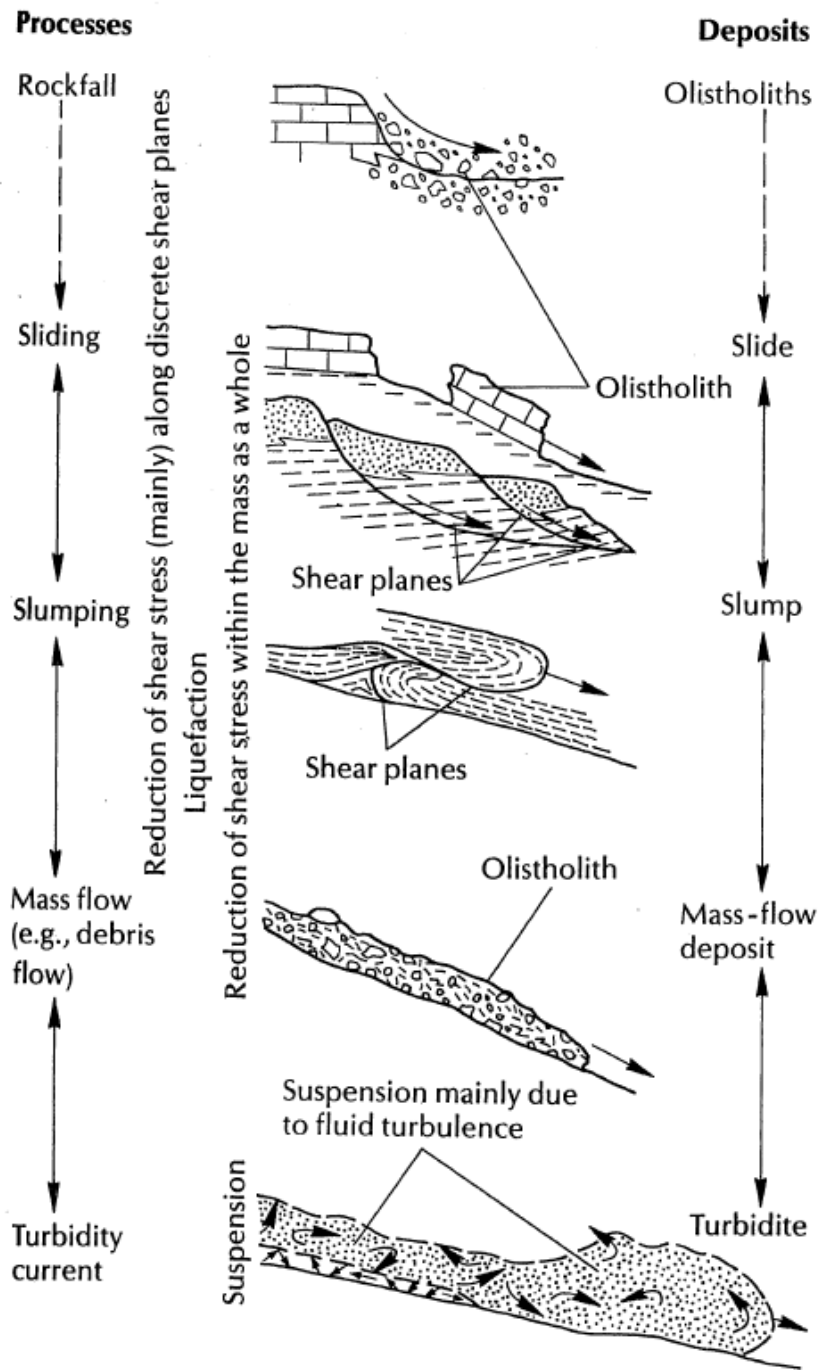
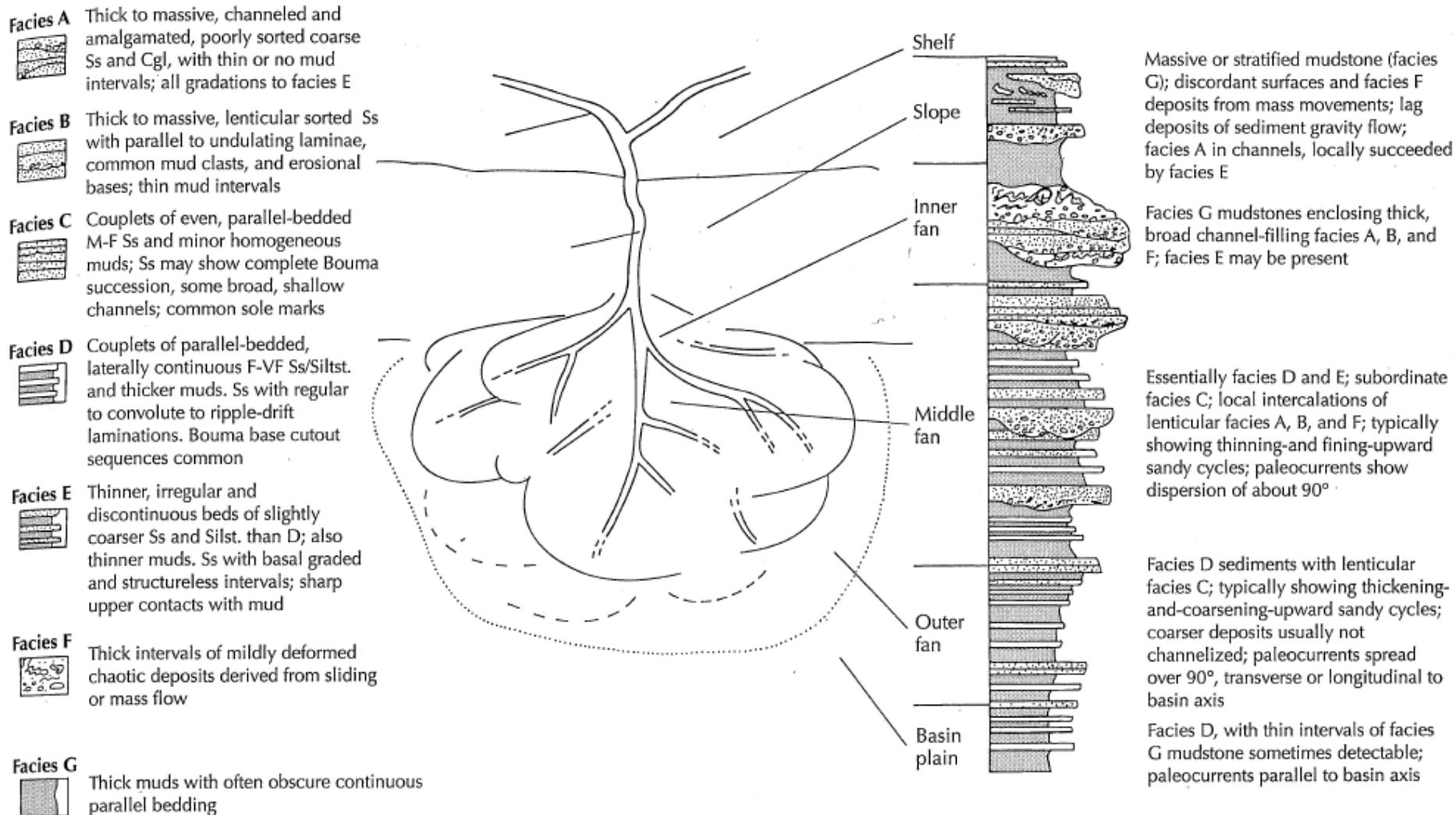
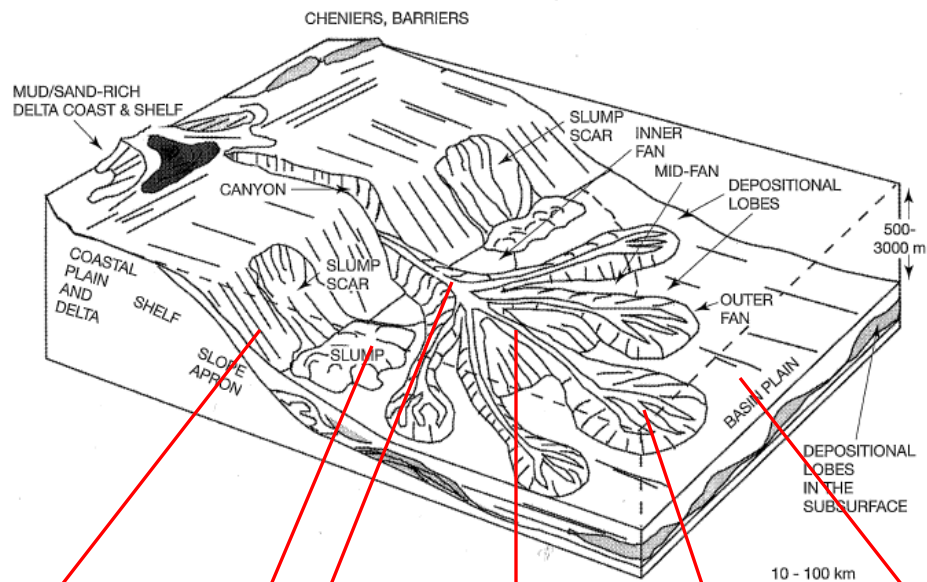


Fig. 10. Allocyclic model of the evolution of a channel-levee system in the lower fan. (A) Phase I: erosion of an elongated valley (Clark and Pickering, 1996). (B) Phase II: relatively coarse-grained sediments (CGS) are deposited within the valley and a narrow channel emerges near the centre. (C) Phase III: depositional process changes from valley-filling to overbanking. (D) Phase IV: decrease in sediment input leads to channel constriction, when inner levees develop. CGS=coarse-grained sediments.



# Submarine Fan Facies



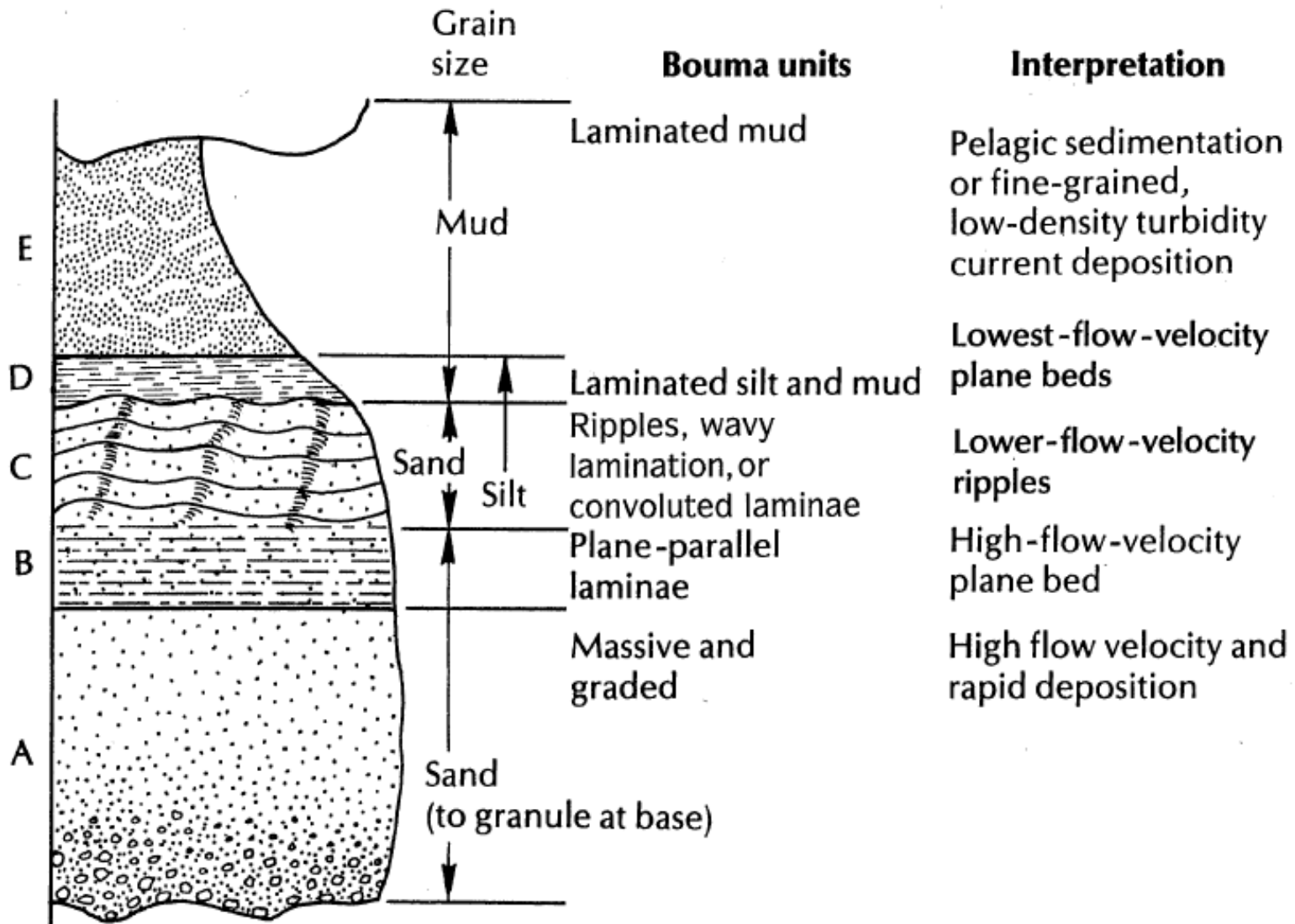


| Facies | Environment |       |        |       | Depositional processes  |       |
|--------|-------------|-------|--------|-------|---|-------|
|        | Slope       | Fan   |        |       |   | Plain |
|        |             | Upper | Middle | Lower |   |       |
| A      |             |       |        |       | Debris flows, liquified flows                                   |       |
| B      |             |       |        |       | Debris flows, liquified flows, turbidity currents (high energy) |       |
| C      |             |       |        |       | Turbidity currents  |       |
| D      |             |       |        |       | Turbidity currents (low energy)                                 |       |
| E      |             |       |        |       | Liquified flows, turbidity currents, traction currents (?)      |       |
| F      |             |       |        |       | Slumps, debris flows  |       |
| G      |             |       |        |       | Pelagic and hemipelagic sedimentation                           |       |

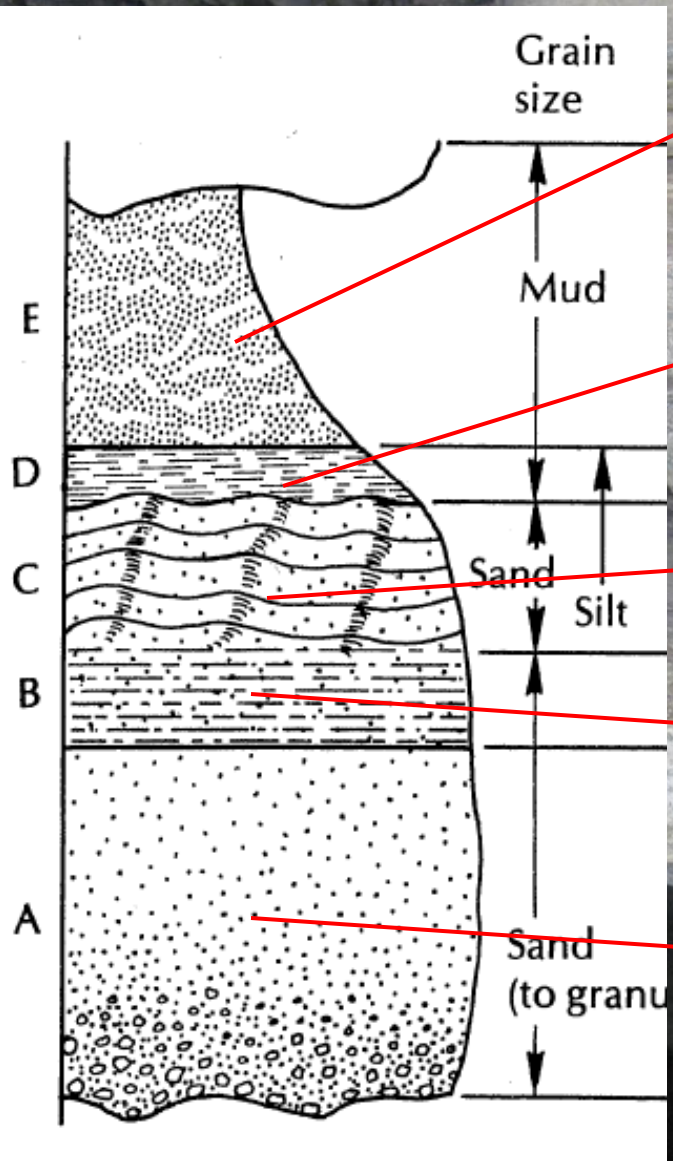
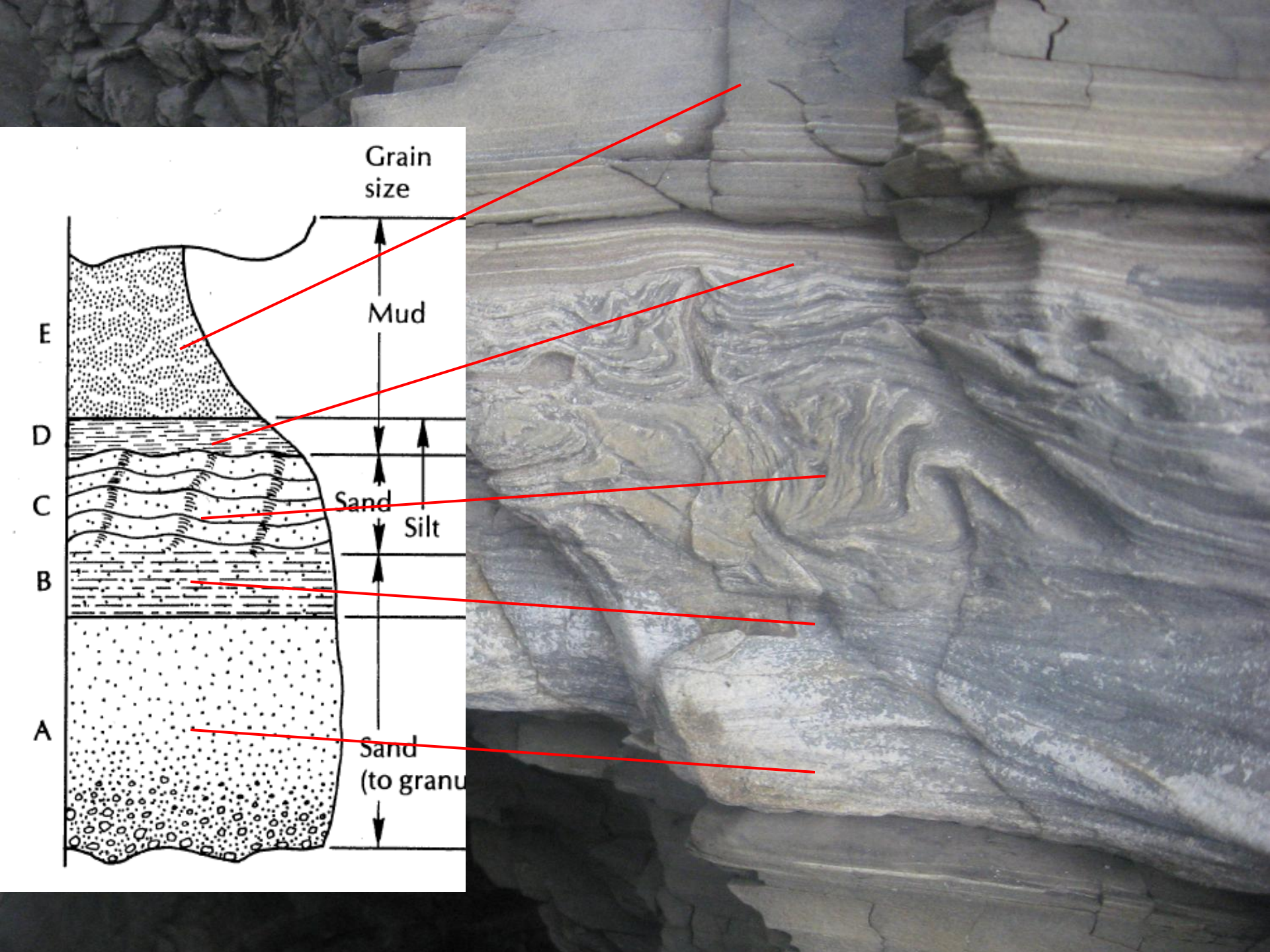




# Bouma Sequences



Commonly scours into previous layer



Not all Bouma layers are likely to be visible in any one place.

The notation for turbidite layers is as follows:

Tabcde: all present

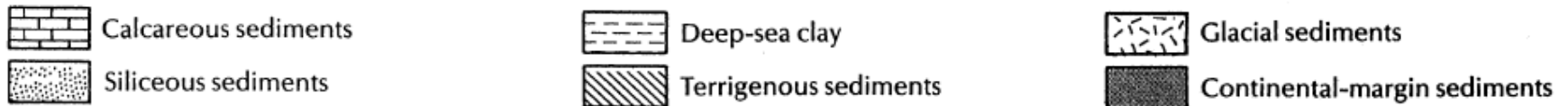
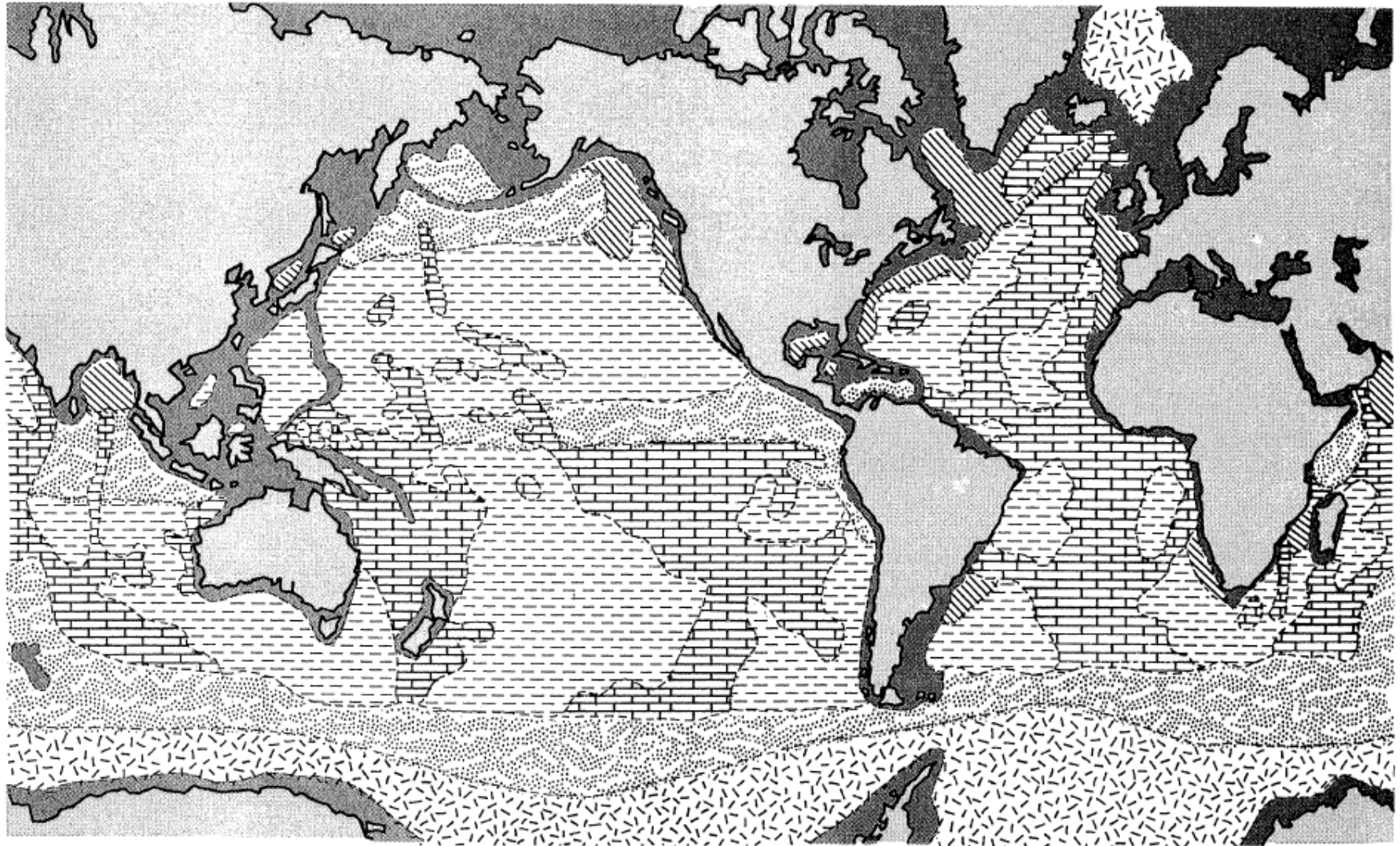
Tacd: only a, c and d present

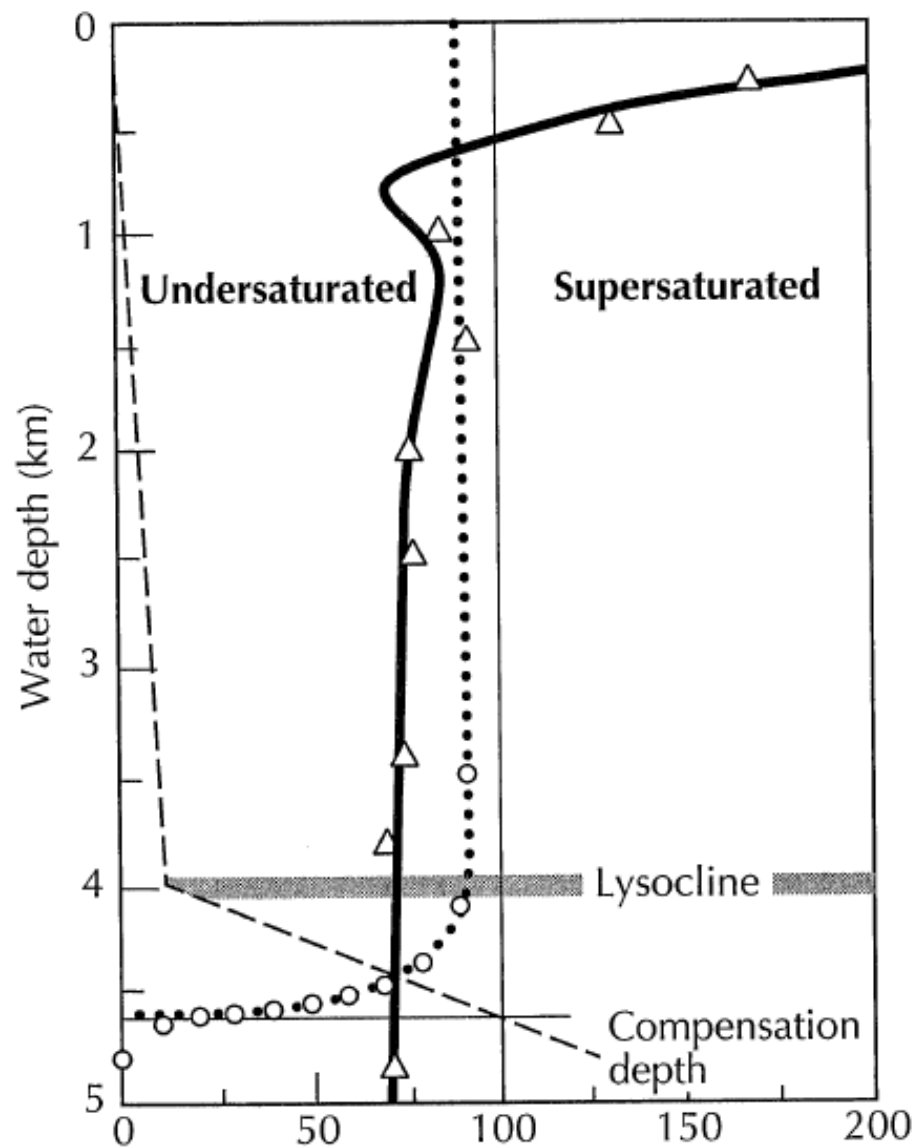
Te: only e present

etc.

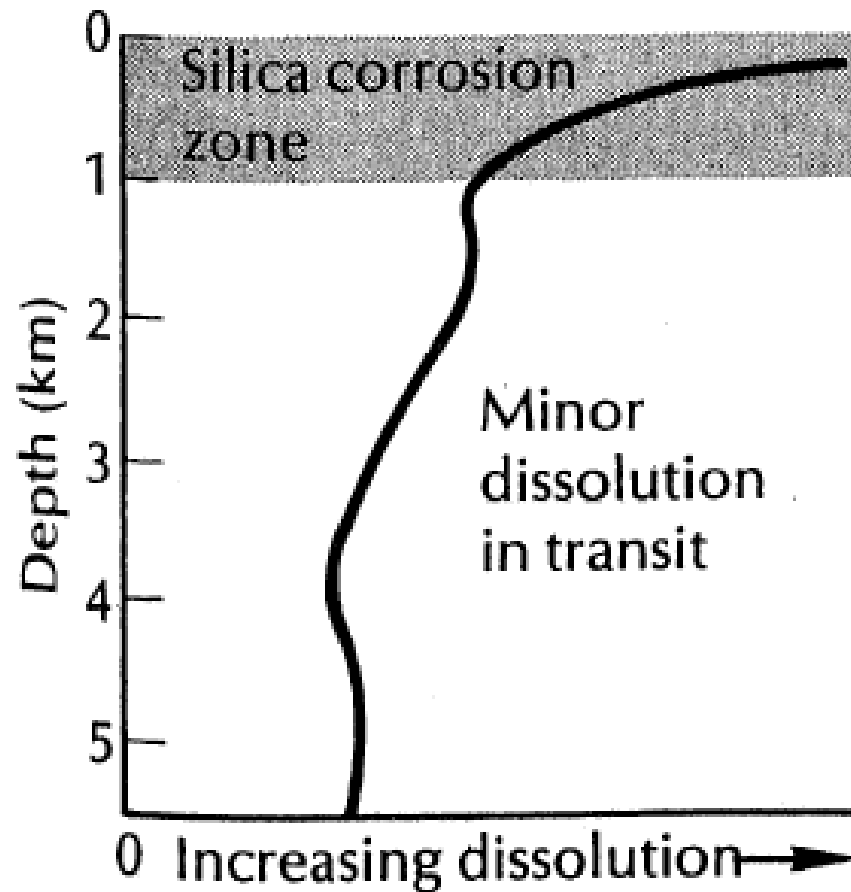


# Deep Ocean Sediments





## Radiolarians



## Foraminifera

